Forward Skirt Structural Testing on the Space Launch System (SLS) Program

J.D. Lohrer[1] and R.D. Wright[2]
Orbital ATK Flight Systems Group, Promontory, Utah

Structural testing was performed to evaluate heritage forward skirts from the Space Shuttle program for use on the NASA Space Launch System (SLS) program. Testing was needed because SLS ascent loads are 35% higher than Space Shuttle loads. Objectives of testing were to determine margins of safety, demonstrate reliability, and validate analytical models. Testing combined with analysis was able to show heritage forward skirts were acceptable to use on the SLS program.

Nomenclature

AE	=	Acoustic Emission
FE	=	Finite Element
FSTA	=	Forward Skirt Structural Test Article
NASA	=	National Aeronautics and Space Administration
SLS	=	Space Launch System
SRB	=	Solid Rocket Booster

I. Introduction

Structural testing was performed to evaluate forward skirts for use on the Space Launch System (SLS) program. These are heritage forward skirts because they were designed and manufactured for use on the Space Shuttle program. Testing was required because SLS ascent loads are approximately 35% greater than Space Shuttle loads.

Forward skirts are part of the Solid Rocket Booster (SRB) as shown in Fig. 1. The purpose of the forward skirt is to transfer thrust from the booster to the core vehicle during flight. This load transfer occurs at the forward attach interface shown in Fig. 2. A ball interface allows only translation loads to be carried and not moments. The highest loads are compressive and reacted through the ball fitting and not the separation bolt depicted. Because of this, the separation bolt was not included in the testing.

Loads reacted at the forward skirt thrust post and ball assembly are shown in Fig. 3. There are two major load events; liftoff and ascent. The liftoff event starts at booster ignition and ends approximately 10 seconds later. The ascent event starts when liftoff ends and continues until separation. Axial loads during ascent increased 35% over shuttle. Radial loads during liftoff increased 68% (inward direction) and 200% (outward direction) over shuttle. Transverse loads did not significantly increase over shuttle. Axial loads are the dominant load despite the fact that radial loads had a larger percentage increase. This is because axial loads are 10 to 20 times greater than radial loads depending on the event.

[1] Design Engineer, Metal and Seals Analysis, Orbital ATK, P.O. Box 707, Brigham City, UT
[2] Technical Lead, Metal and Seals Analysis, Orbital ATK, P.O. Box 707, Brigham City, UT

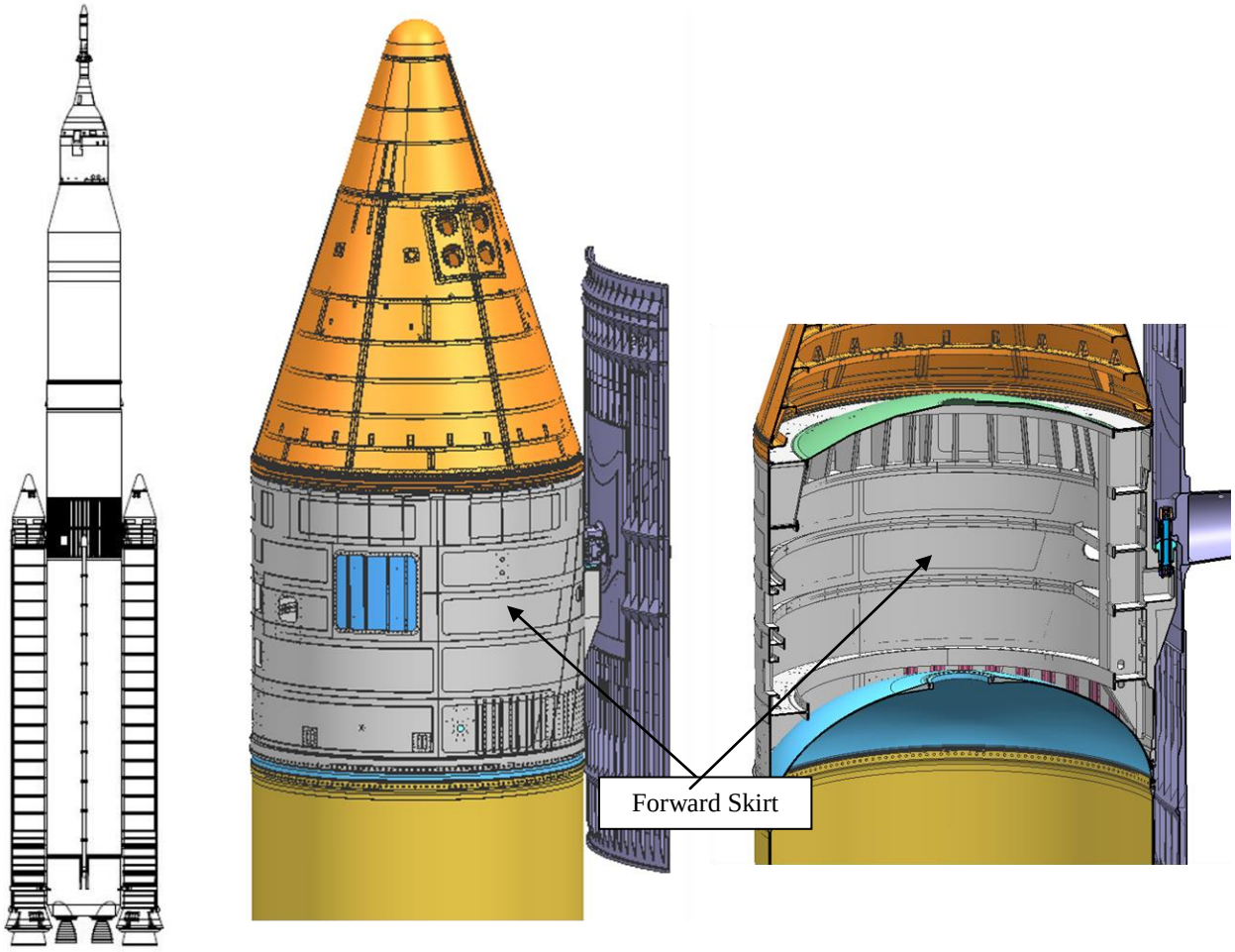

Figure 1. SLS Vehicle and Forward Skirt.

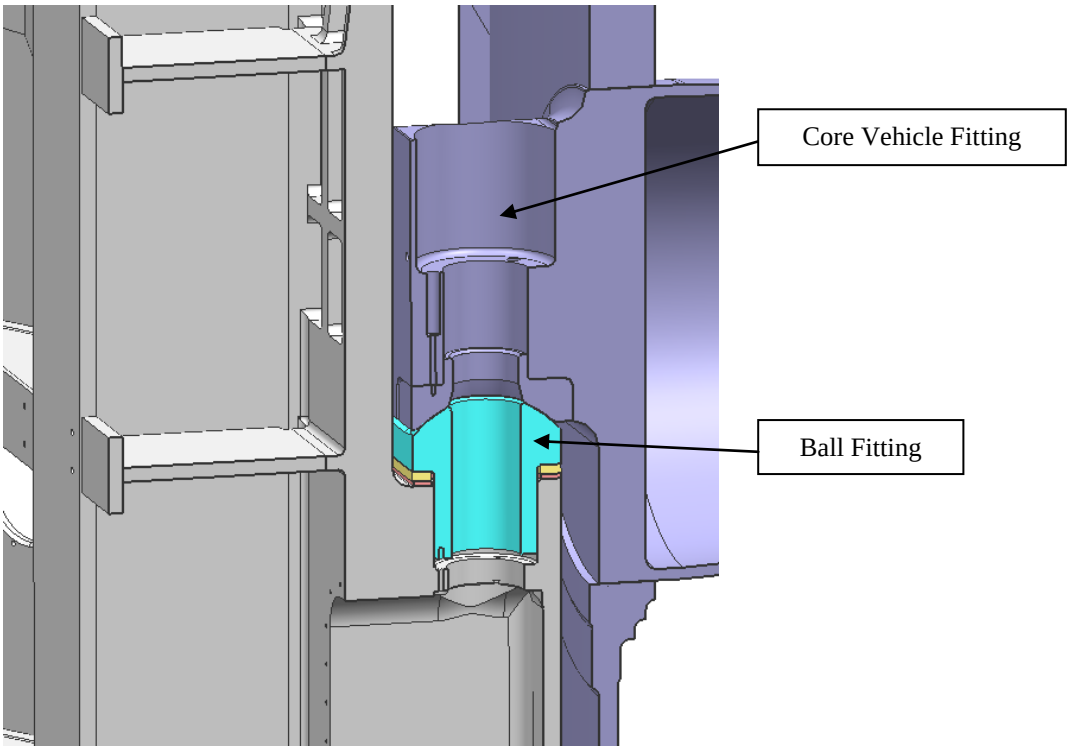

Figure 2. Forward Attach Interface.

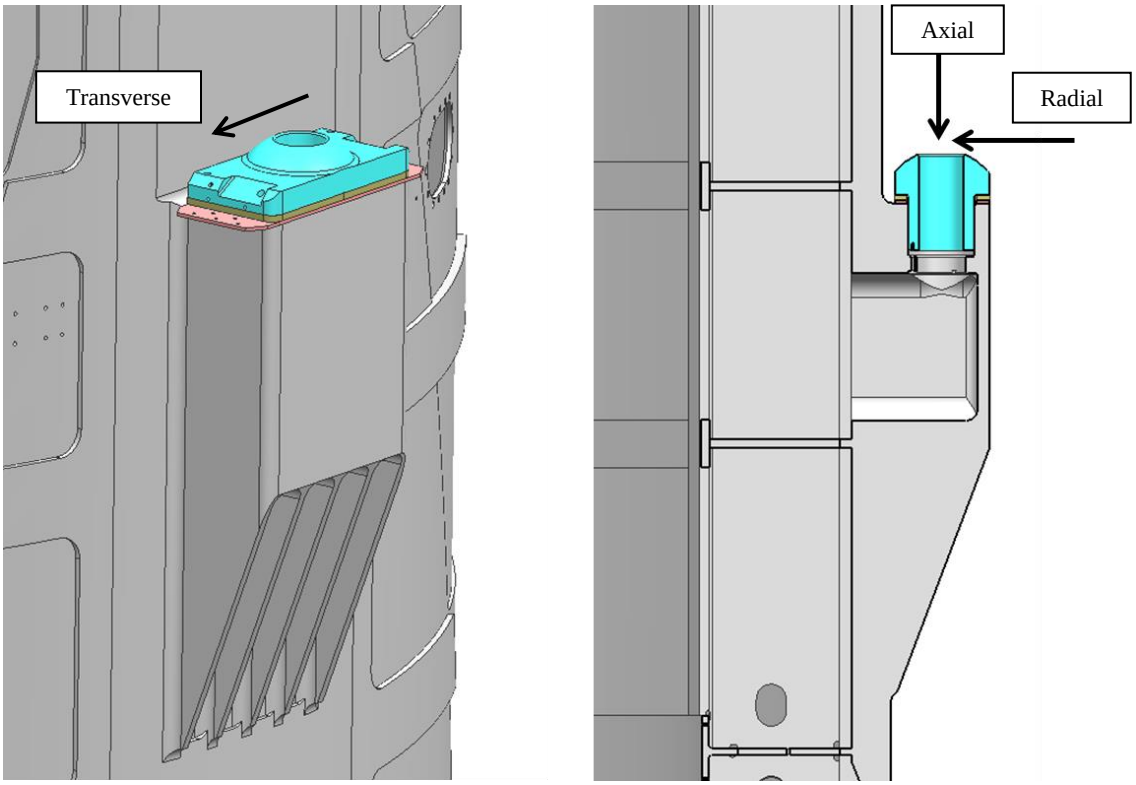

Figure 3. Forward Skirt Loads.

The forward skirt consists of aluminum 2219 parts welded together as shown in Fig. 4. Three skin panels, two ring forgings, a thrust post forging, and internal rings are the main parts of the forward skirt. Stringers were not part of the heritage design. Stringers are bolted to the skin in the aft region to increase the buckling capability because of higher SLS loads. A close-up view of the thrust post is shown in Fig. 5. The lowest material strength occurs in the thrust post forging.

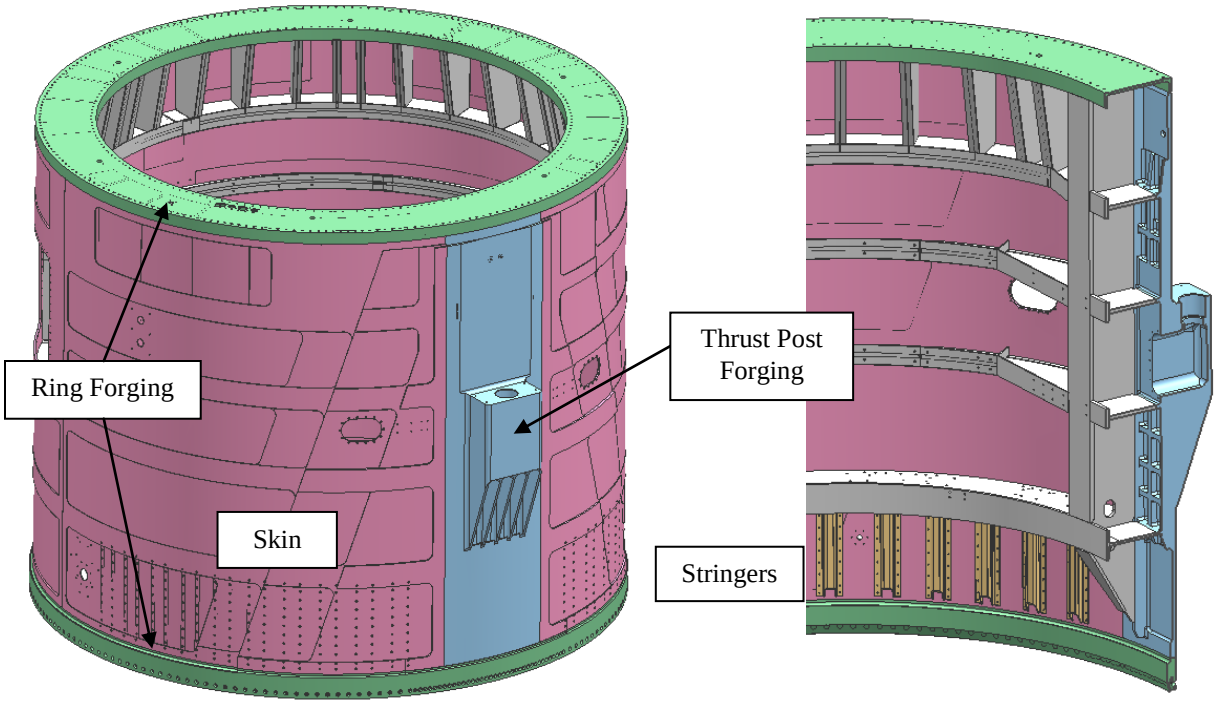

Figure 4. SLS Forward Skirt.

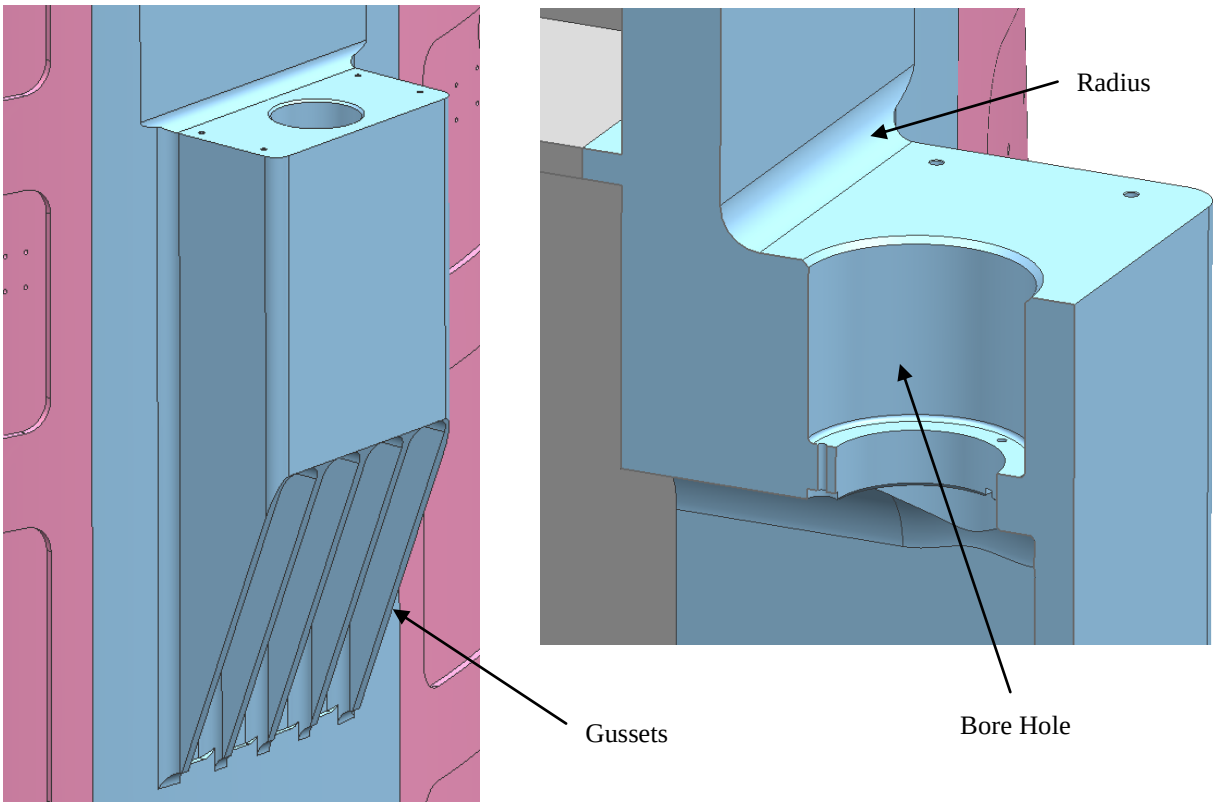

Figure 5. SLS Forward Skirt Thrust Post.

II. Test Description

Testing was performed at Orbital ATK facilities in Promontory, Utah. The test setup is shown in Fig. 6. The test stand applied loads to the forward skirt are shown in Fig. 7. Four hydraulic actuators were used to apply axial load and two hydraulic actuators were used to apply radial and tangential loads. Four load cells measured axial loads while load cells were built into the hydraulic actuators that applied lateral loads.

Figure 6. Test Setup.

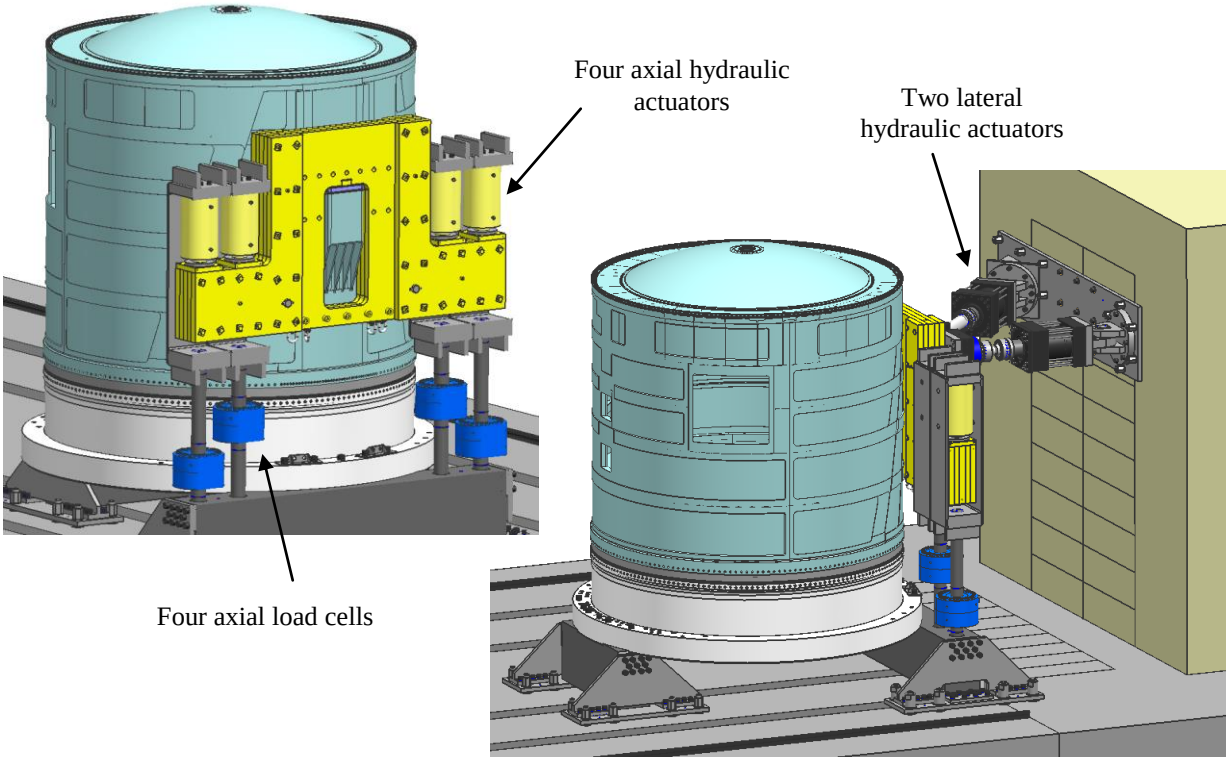

Figure 7. Test Stand Load Application.

The first test was referred to as FSTA-1 and was performed in April/May 2014. The purpose of FSTA-1 was to verify the ultimate capability of the forward skirt subjected to ascent loads. Testing consisted of two liftoff load cases taken to 100% load followed by an ascent load case taken to 110% load. The forward skirt was unloaded to no load after each test case. A final ascent loading was applied to 140% followed by increasing the ascent load until failure occurred.

The second test was referred to as FSTA-2 and performed in July/August of 2014. The purpose of FSTA-2 was to verify the ultimate capability of the forward skirt subjected to liftoff loads. Testing consisted of six liftoff load cases taken to 100% load followed by the six liftoff cases taken to 140% load. Two ascent load cases were then tested to 100% limit load. The forward skirt was unloaded to no load after each test case. A final ascent loading was applied to 140% followed by increasing the ascent load until failure occurred.

III. Test Results

The forward skirts on FSTA-1 and FSTA-2 successfully carried all applied liftoff and ascent load cases. Both FSTA-1 and FSTA-2 were tested to failure by increasing the ascent loads. Failure occurred in the forward skirt thrust post radius as shown in Fig. 8 and 9. The forward skirts on FSTA-1 and FSTA-2 had nearly identical failure modes. FSTA-1 failed at 1.72 times limit load and FSTA-2 failed at 1.62 times limit load. This difference is primarily attributed to variation in material properties in the thrust post region.

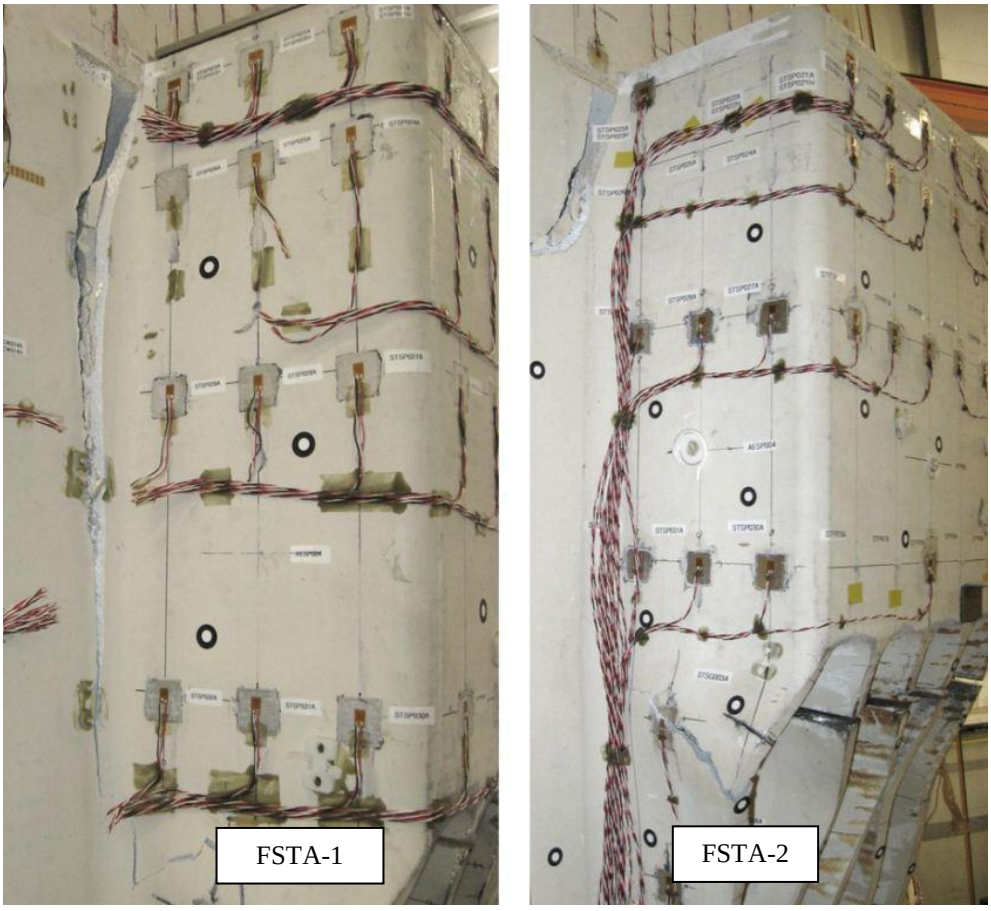

Figure 8. Side View of Post Failure.

*

Figure 9. Top View of Failure.

Test data were obtained from strain gages, deflection gages, ARAMIS optical strain measurement system, Acoustic Emissions (AE), and high-speed video. Strain gage data and ARAMIS strain were compared to Finite Element (FE) analysis predictions. The FE model shown in Fig. 10 and 11 was used in the analyses. Both the forward skirt and test stand tooling was modeled. This allows the analysis to simulate the loading as close as possible to the actual test configuration.

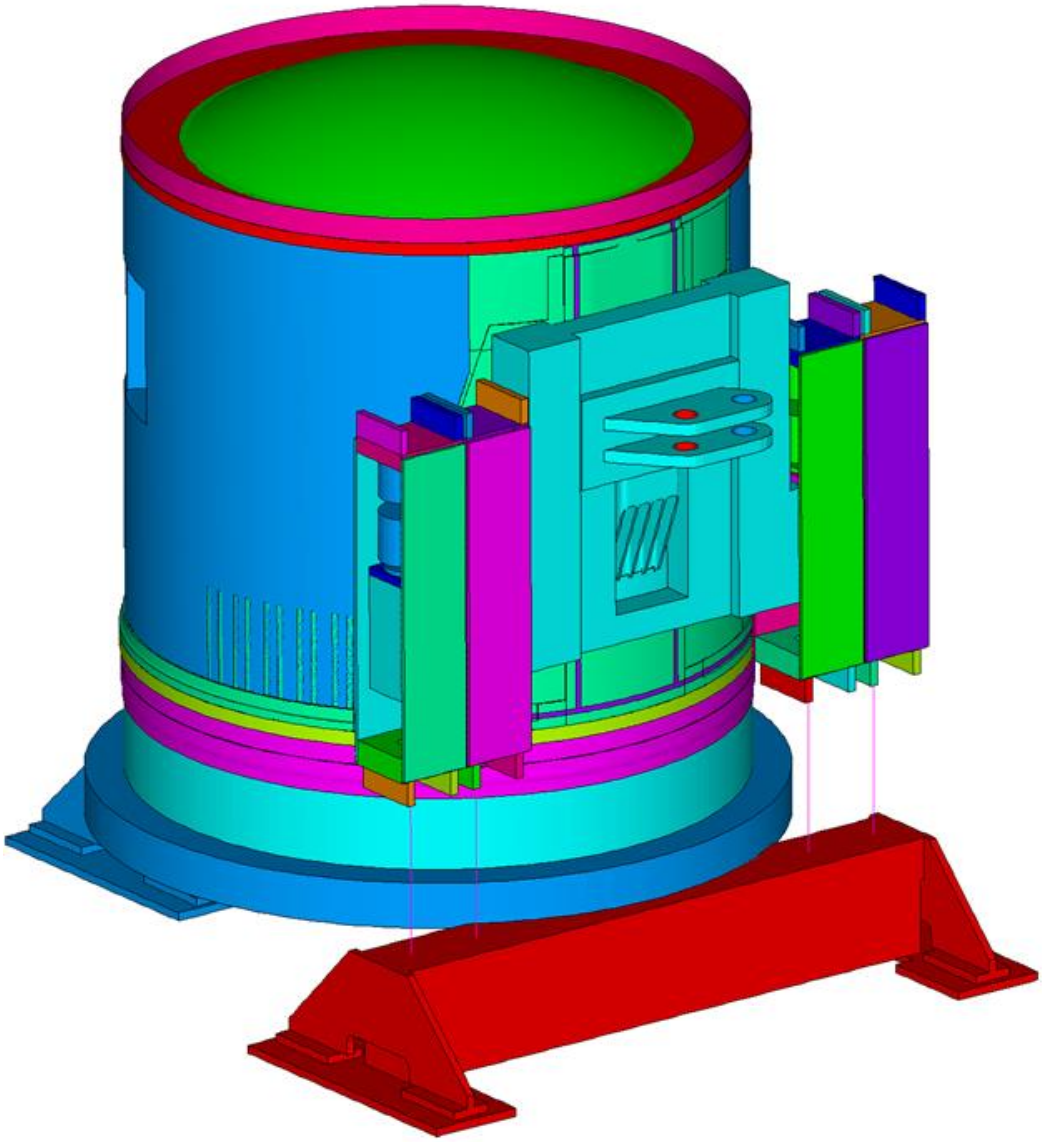

Figure 10. FSTA Finite Element Model.

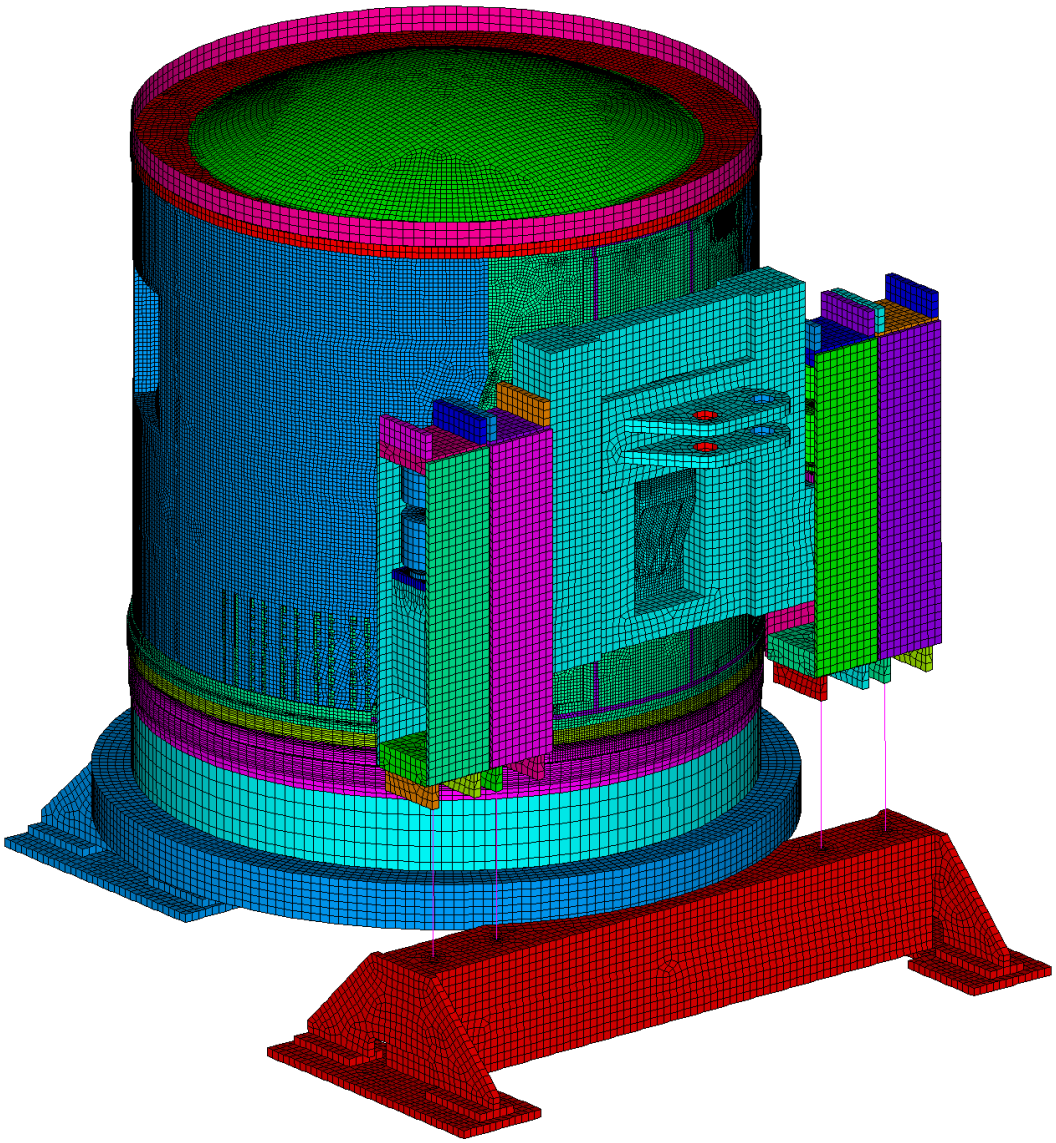

Figure 11. FSTA Model Mesh Density.

A. Strain Gage Data

FSTA-1 and FSTA-2 were instrumented with over 200 strain gages to ensure all possible failure modes could be captured. However, it turned out that three gages provided the most useful strain data. One was located in the post bore and two on the post radius as shown in Fig. 12. Measured strains were compared to analysis results for the final loading as shown in Fig. 13 through 16. The FSTA-1 post radius gage responses enveloped the nominal analytical prediction in Fig. 13 and the post bore gage showed excellent correlation with the analytical prediction for the loading and unloading cycles in Fig. 14. Note that FSTA-1 gages were lost before failure was reached. FSTA-2 gages survived to the failure load but one of the radius gages was lost before testing began. This gage was not replaced because of the time and cost associated with disassembly of the test structure and redundancy of the ARAMIS system. FSTA-2 analysis correlation was not quite as good because there was more residual strain effects from the load cycles previously applied. FSTA-2 was loaded and unloaded with 12 liftoff cases and two ascent cases before taking the skirt to failure. FSTA-1 only had two liftoff cases and one ascent case before taking the skirt to failure.

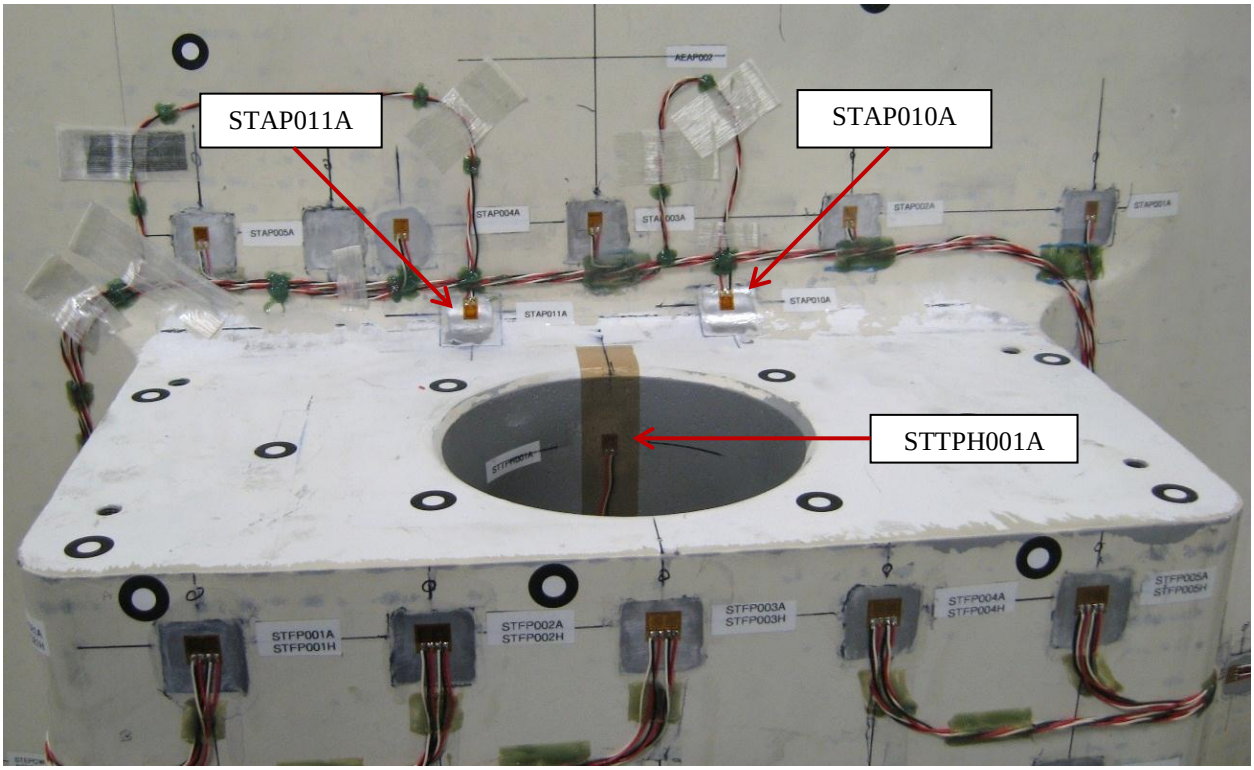

Figure 12. Critical Strain Gages.

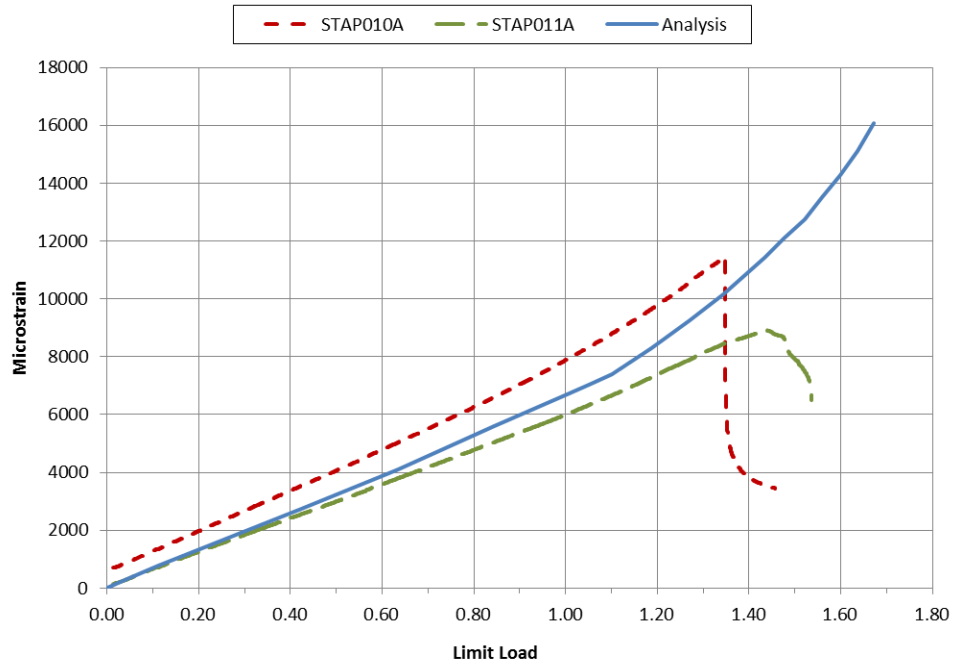

Figure 13. FSTA-1 Radius Gage Strains.

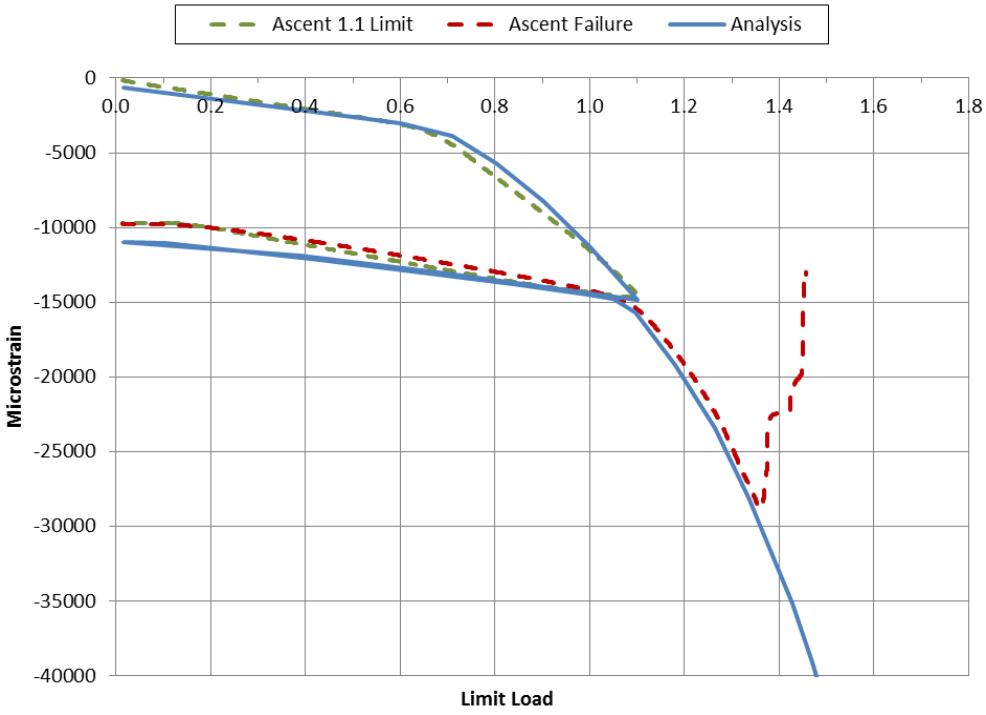

Figure 14. FSTA-1 Bore Gage Strains.

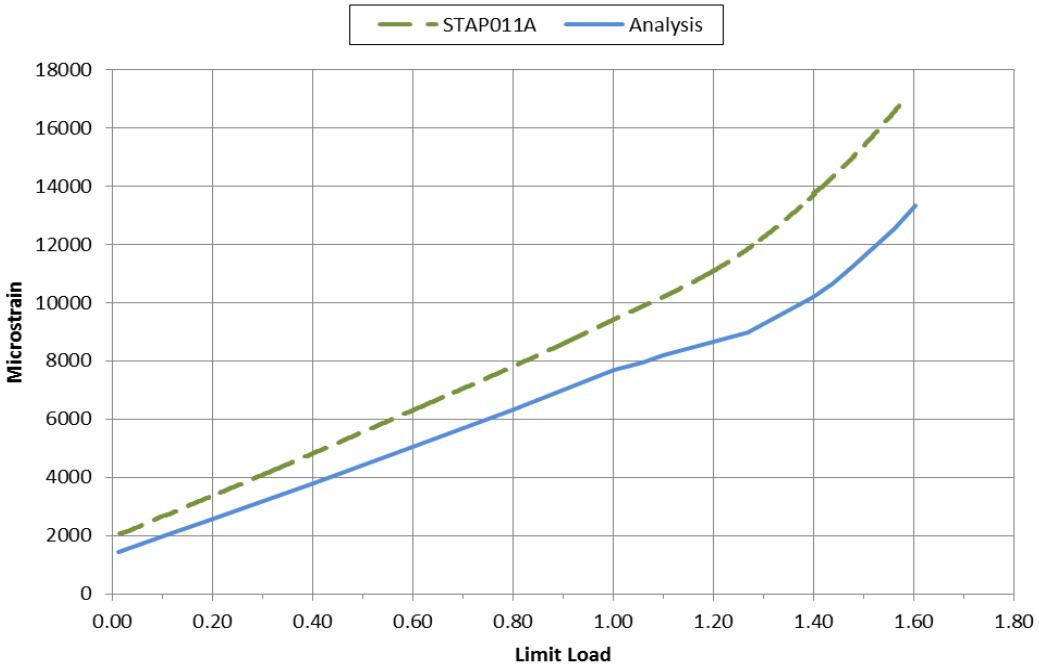

Figure 15. FSTA-2 Radius Gage Strains.

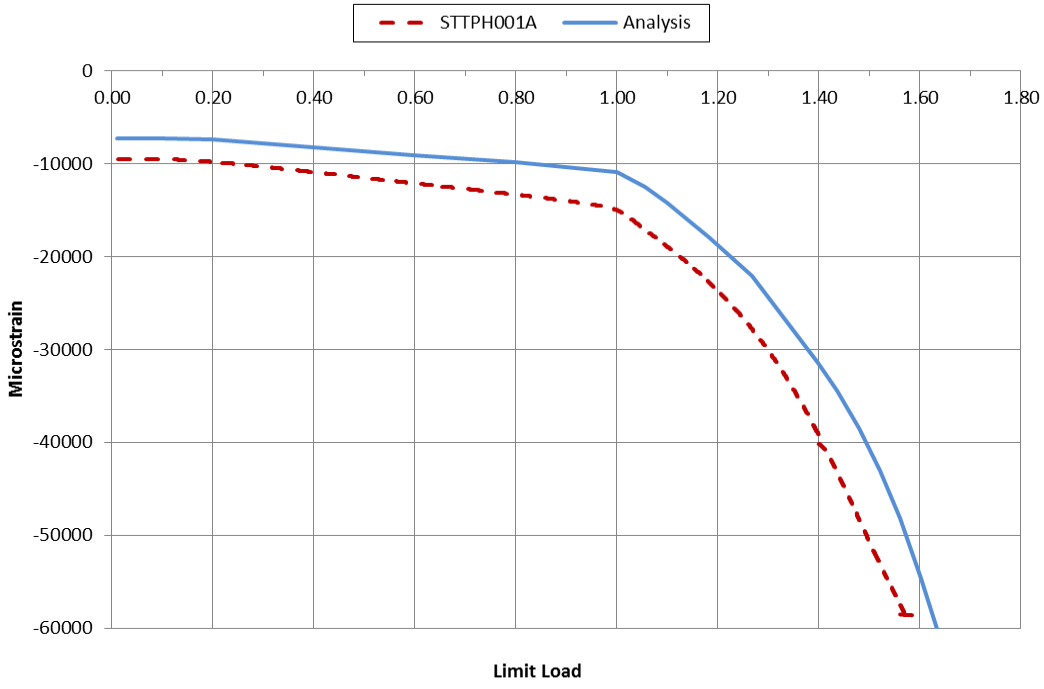

Figure 16. FSTA-2 Bore Gage Strains.

B. ARAMIS Data

Strain at the post radius was determined by processing digital images with the ARAMIS system. A speckled paint pattern was required on the post radius as shown in Fig. 17. Digital cameras were mounted at the top of the forward skirt as shown in Fig. 18. This was not the most desirable setup but was required to avoid tooling used to apply loads. Even with this limitation, ARAMIS was able to accurately capture the thrust post strain. ARAMIS strain results are shown in Fig. 19 for FSTA-2 just prior to failure. A high strain develops near the left side. This high strain compares well to analysis prediction for both FSTA-1 and FSTA-2 as shown in Fig. 20. The strain at this location was also plotted versus load in Fig. 21 and 22. Both FSTA-1 and FSTA-2 had excellent correlation between ARAMIS and analysis strains.

Figure 17. Post Radius Speckle Pattern.

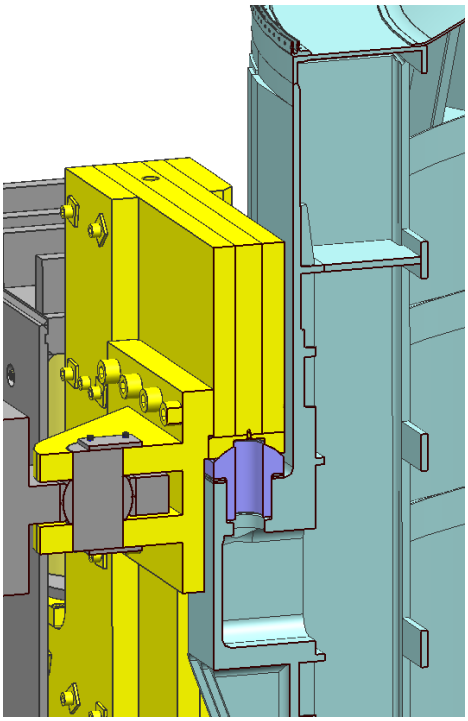

Figure 18. ARAMIS Digital Cameras.

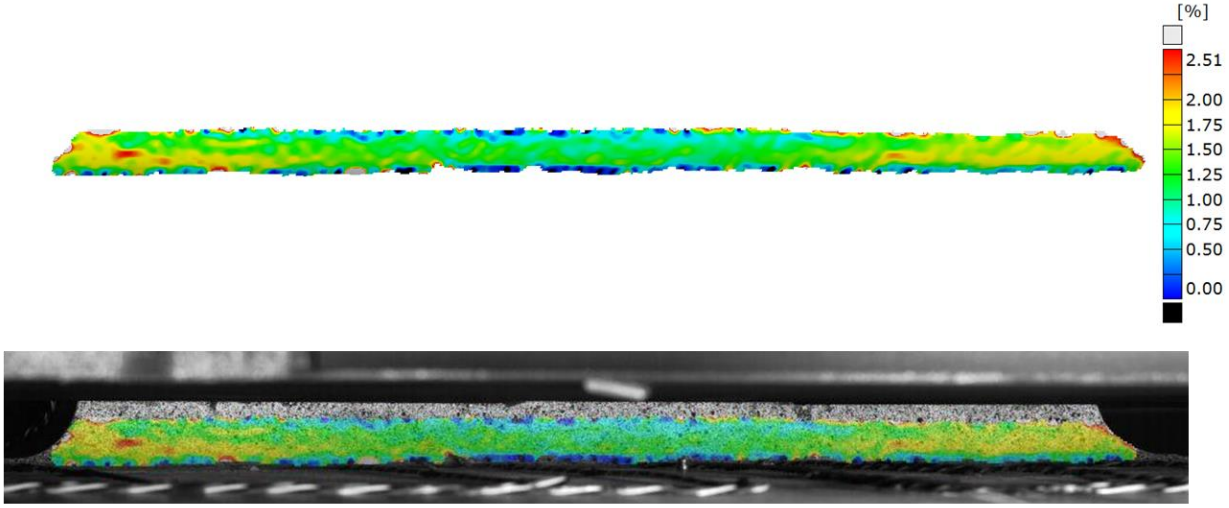

Figure 19. FSTA-2 ARAMIS Strain prior to Failure.

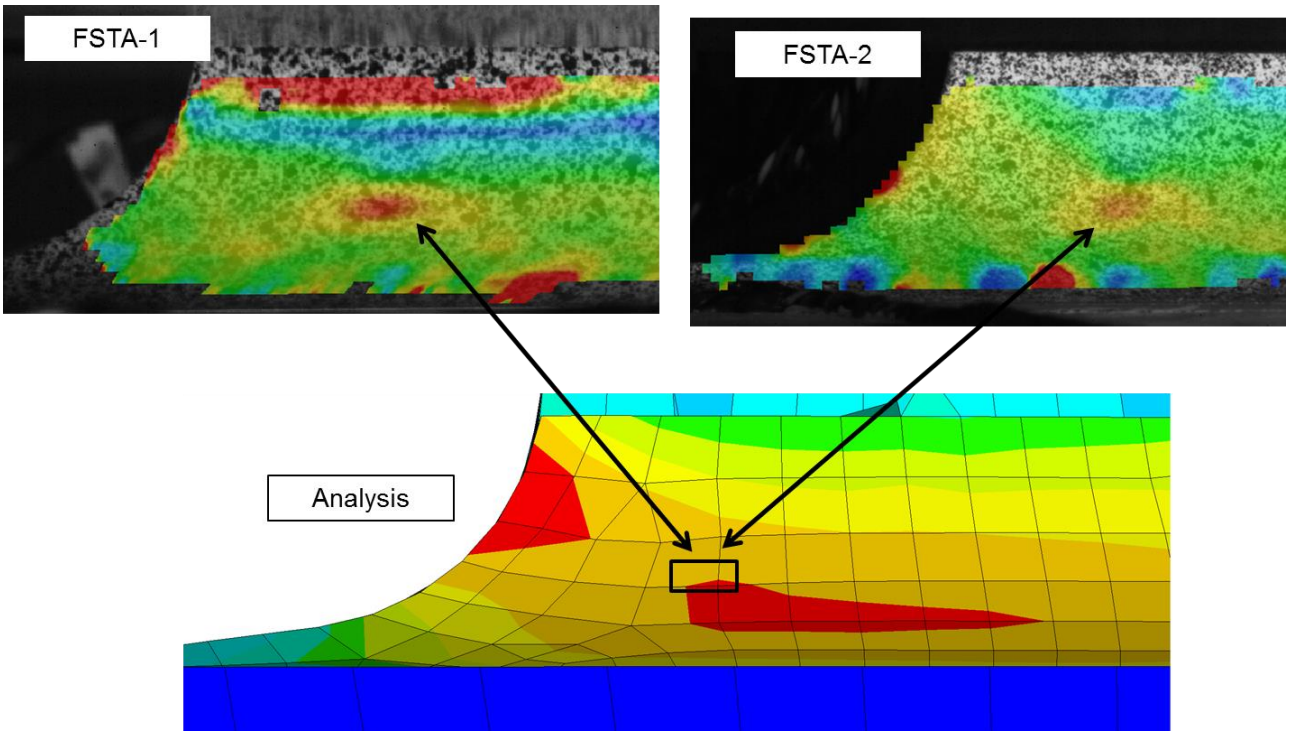

Figure 20. ARAMIS versus Analysis Strain at Hot Spot.

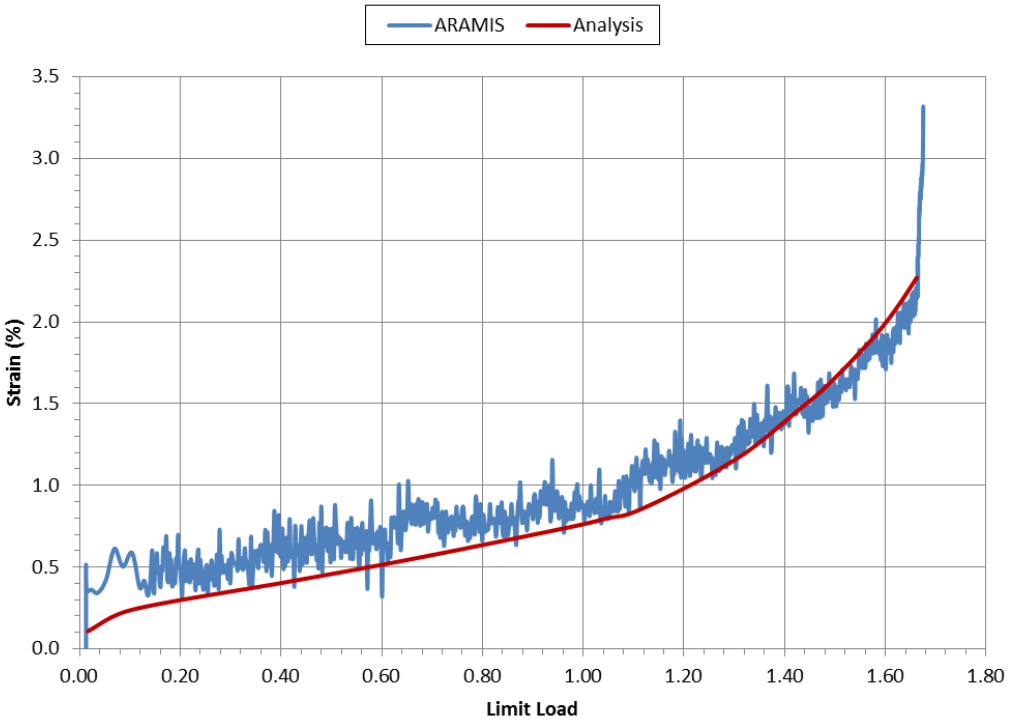

Figure 21. FSTA-1 ARAMIS versus Analysis Strain.

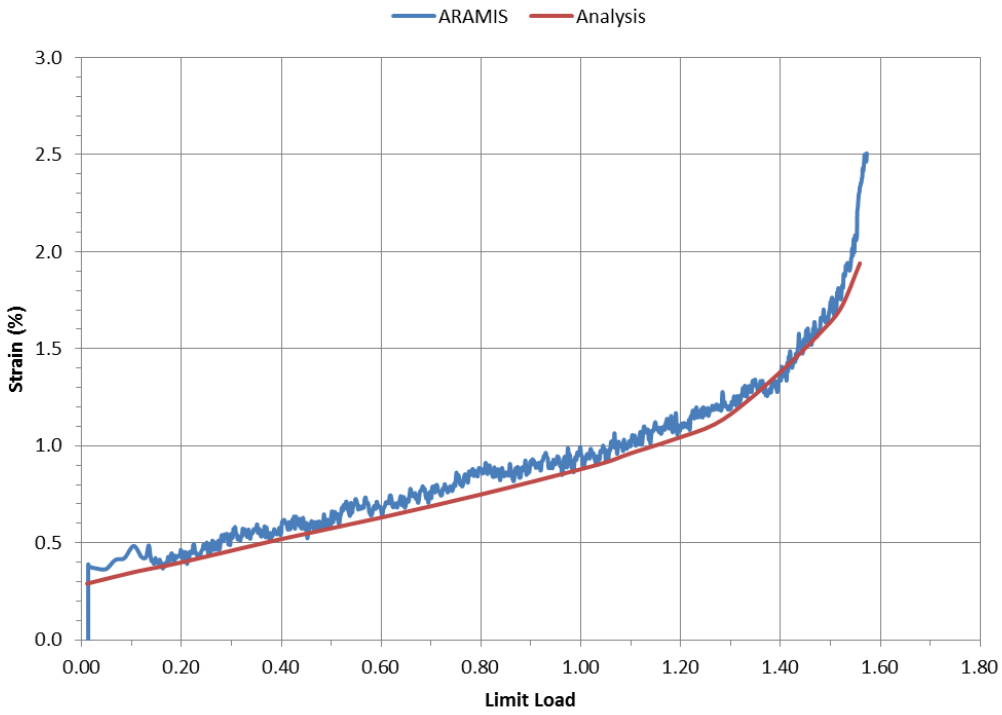

Figure 22. FSTA-2 ARAMIS versus Analysis Strain.

C. Acoustic Emission Data

AE sensors were used to monitor for damage formation that may occur during testing (e.g. crack formation and growth). AE was important because after disassembly of FSTA-1, a crack was observed in the ball fitting radius as shown in Fig. 23. The ball fitting did not crack on FSTA-2. AE data were used to reconstruct when the crack occurred. This was essential in determining the ball fitting margin of safety. The AE energy versus time plot for FSTA-1 is shown in Fig. 24. The energy increased considerably at 850 seconds (152% limit load), indicating a crack could have formed at this point. The only visual evidence found from standard and high- speed video that could have corresponded to this event was the crack that initiated in the ball fitting.

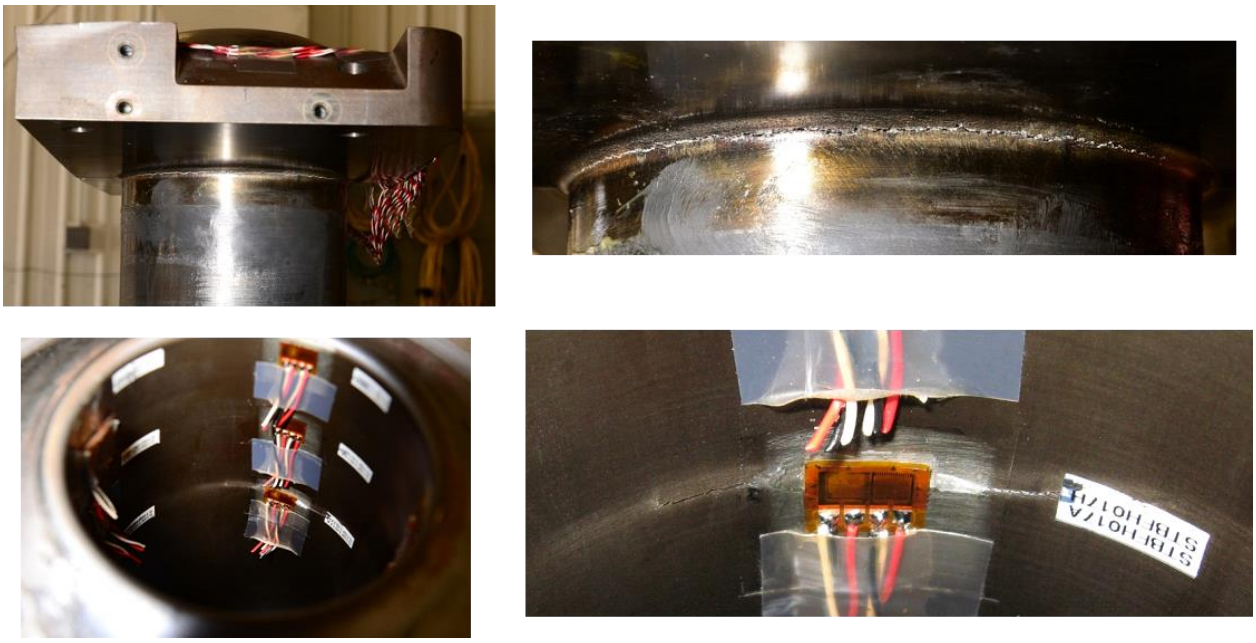

Figure 23. Crack at Ball Fitting Radius on FSTA-1.

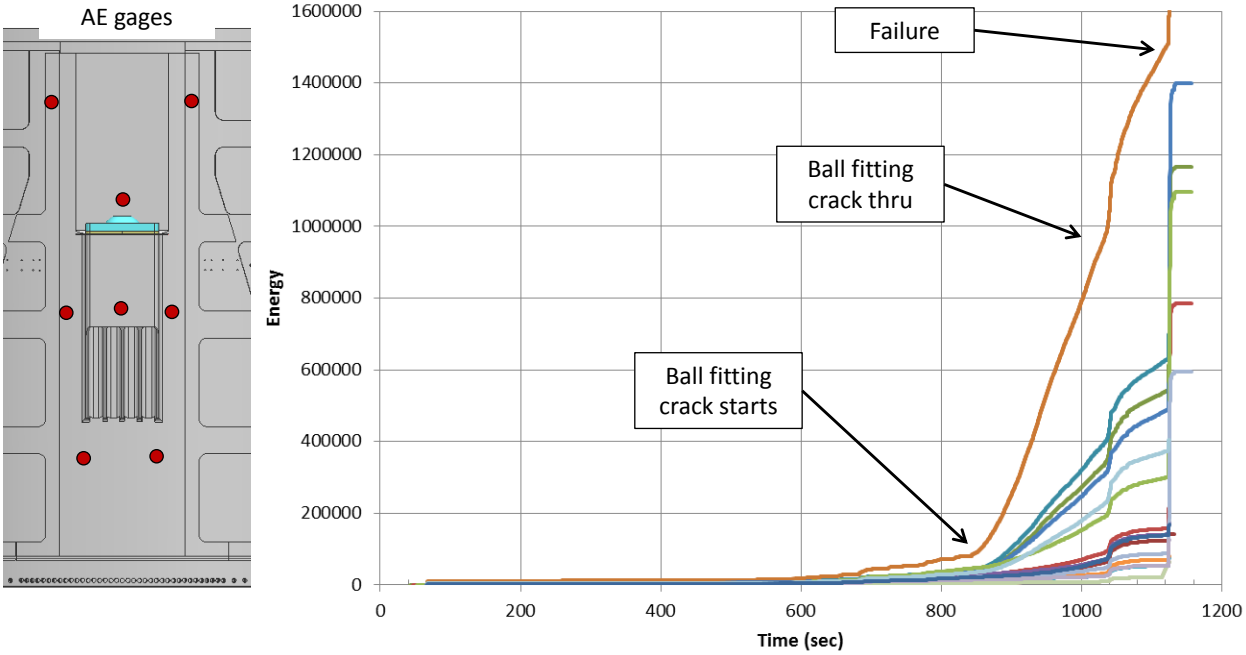

Figure 24. FSTA-1 Acoustic Energy Events.

IV. Conclusion

In summary, testing of the heritage forward skirts was a success. Testing combined with analytical correlation helped show the forward skirts were acceptable to use on the SLS program. This saved the SLS program approximately 30 million dollars because new forward skirts did not have to be designed, tested, and manufactured.